Actualizing In Situ X-ray Absorption Spectroscopy Characterization of PEMFC-Cycled Pt-Electrodes

Todd E. Miller,[1] Veronica Davies,[1] Jingkun Li,[1] Shraboni Ghoshal,[1] Eli Stavitski,[2] Klaus Attenkofer,[2] Sanjeev Mukerjee,[1,*] and Qingying Jia[1,z]

[1]*Department of Chemistry and Chemical Biology, Northeastern University, Boston, Massachusetts 02115, USA*
[2]*National Synchrotron Light Source II, Brookhaven National Laboratory, Upton, New York 11973, USA*

The family of the PtM (M represents transition metals such as Co, Ni, Pd, etc.) alloys is the most promising cathode electrocatalysts for proton exchange membrane fuel cells (PEMFCs) owing to their superior oxygen reduction reaction (ORR) activity to pure Pt. However, the activity gain fades with long-term PEMFC operation, and the degradation mechanism is not yet fully understood. To truly understand the degradation mechanism of the carbon supported PtM nanoparticles (PtM/C) in the cathode of a membrane electrode assembly (MEA) upon long-term PEMFC operation, it is essential to characterize the *PEMFC-cycled* electrode under working conditions. Herein, we showed that operando X-ray absorption spectroscopy (XAS) characterization of PtM/C electrocatalysts cycled in a PEMFC has inherent difficulties since Pt and especially M dissolve during PEMFC operation and migrate into the membrane; the bulk XAS spectrum is an average of the signals from the electrode and the membrane. Alternatively, we developed a method that allows for in situ XAS characterization on *PEMFC-cycled* PtM/C electrocatalysts. We justified the method by showing that the dissolved species in the membrane were separated from the PtM/C electrocatalyst in the cathode, and the in situ XAS signals arose exclusively from the electrocatalyst.

 [DOI: 10.1149/2.0151809jes]

Manuscript submitted December 4, 2017; revised manuscript received May 14, 2018. Published May 26, 2018.

Despite recent progress in the development of non-platinum electrocatalysts for the oxygen reduction reaction (ORR), carbon supported platinum-based nanoparticles (NPs) are still so far the only viable electrocatalysts for practical proton exchange membrane fuel cells (PEMFCs) in automotive vehicles, owing to their high activity and durability under the highly oxidative and corrosive conditions in the cathode of a PEMFC. The ORR activity of platinum can be significantly improved by alloying Pt with a wide range of transition metals (denoted as M) such as Co, Ni, Y, and the activity improvement has been attributed to the strain and/or ligand effects induced by M via optimization of the Pt-O binding energy and surface coordinate configuration.[1–5] However, the activity gain induced by M is generally not sustainable owing primarily to the dissolution of M during long-term PEMFC operation, which leads to the attenuation of strain/ligand effects, particle growth, and the loss of the favorable surface coordinate configuration.[6] Huang et al.[7] recently reported that both the activity and durability of the PtNi/C octahedral NPs can be markedly improved by doping with a transition metal such as Mo on the surface. However, neither the degradation mechanism of the PtM/C electrocatalysts during long-term PEMFC operation, nor the corresponding alleviation mechanism, is fully understood, which limits further improvements of the PtM/C electrocatalysts for PEMFCs.

Elucidating the degradation mechanism of the PtM/C electrocatalysts during long-term PEMFC operation is technically challenging as it requires proper electrochemical testing methods and characterization methods, and a combination thereof. A regular way is to potentially cycle the PtM/C electrocatalyst in a rotating disk electrode (RDE) following certain protocols, and measure the structure and composition of the PtM/C NPs at different cycling stages. This method provides insightful information of the structure evolution of the PtM/C NPs with the potential cycling. However, the electrochemical environment between a RDE and a PEMFC is drastically different, and the modes of the evolution of the structure of the PtM/C NPs, the Pt and M dissolution and aggregation established in a RDE are not fully representative of the modes of the PtM/C NPs in a PEMFC.[8] In addition, the structure of the PtM/C NPs acquired by ex situ characterizations may also not be highly relevant to the catalytic activity as it often differs from that under in situ working conditions. In situ spectroscopic and/or microscopic studies of the degradation mechanism of PtM/C electrocatalysts have been implemented by using an in situ electrochemical half-cell, but it has the same issue of the RDE system aforementioned as the electrochemical environment of a half-cell does not closely resemble that of a PEMFC. To truly understand the degradation mechanism of the PtM/C NPs in the cathode of a membrane electrode assembly (MEA) subject to long-term PEMFC operation, it is essential to characterize the *PEMFC-cycled* electrodes under in situ conditions to monitor the real-time structure evolution of the PtM/C NPs.

X-ray absorption spectroscopy (XAS) empowered by synchrotron-based X-ray with high flux has unique advantages in characterizing the electrocatalysts buried in the sandwich configuration of a MEA in the complex environments of a PEMFC. In addition, XAS is extremely suitable for understanding the structural and mechanistic basis of the ORR activity and durability of PtM/C electrocatalysts since it allows for quantitative evaluation of the strain, ligand, particle size, and site-blocking effects on their catalytic performance.[5,6,9–11] Therefore, substantial efforts have been devoted to actualizing in situ/operando XAS characterization of PtM/C NPs cycled in PEMFCs to obtain the structure-activity-durability correlations.[12,13] An operando XAS fuel cell was built wherein the MEA was composed of a cathode electrode of PtNi/C NPs subject to XAS characterization, and an anode electrode of Pd/C NPs (the Pt/C NPs cannot be used due to the convolution of the Pt signals from the Pt/C and the PtNi/C). However, Ni oxides were detected even at the very early stage of the operation, which indicated the dissolution of the Ni from the electrode and migrate into the membrane.[12] Similarly, Cobalt oxides were observed using the same operando cell with PtCo/C as the cathode electrocatalyst.[14] While the operando XAS measurement clearly showed the dissolution of M, it provided little information of the morphology of the PtM/C NPs since the XAS spectra is an average of signal from the electrodes, the membrane, and the ionomer owing to its bulk average nature. Since the dissolution of Pt and especially M from the electrode and the subsequent migration into the membrane during long-term PEMFC operation are inevitable, operando XAS characterizations on the PEMFC-cycled PtM/C electrocatalysts are technically challenging. In addition, the configuration of non-Pt anode does not ideally resemble that of the MEA normally associated with Pt anode in a practical PEMFC.

In this work, we overcame the practical difficulty of XAS by developing a new method to actualize in situ XAS characterizations on the *PEMFC-cycled* PtM/C electrocatalysts. The morphology evolution of the PtNi/C NPs during long-term PEMFC operation acquired by this method correlated well with the ORR performance obtained

*Electrochemical Society Fellow.
[z]E-mail: q.jia@neu.edu

in practical PEMFCs. This method can be extended to many other spectroscopic techniques.

Experimental

Catalyst and MEA preparation.—The PtCo/C[5] and dealloyed PtNi/C[15] catalysts were synthesized via a typical route as fully described elsewhere. The MEAs with the PtCo/C as the cathode electrocatalyst were fabricated by a typical catalyst-coated membrane (CCM) method, wherein the catalyst layers were coated on the surface of polymer electrolyte membrane so it was sandwiched between two electrodes. The Pt loading of the cathode PtCo electrode and anode Pt/C was 0.2 mg_{Pt} cm^{-2} and 0.05 $mg_{Pt} \cdot cm^{-2}$, respectively, and the I/C ratio was 0.6. The 50 cm^2 cathode- and anode-catalyst-coated decals were then hot pressed onto a 25 μm Nafion-111 membrane (NRE211, 1100 EW, DuPont) at 140°C.

The MEAs with the PtNi/C[15] as the cathode electrocatalyst were fabricated by a catalyst-coated diffusion media (CCDM) method,[16] wherein the electrocatalysts were coated onto the microporous layer rather than the membrane like the CCM method. An ionomer layer was then sprayed on the catalyst layer. Afterwards, the CCDM anode was hot-pressed into the membrane; whereas the cathode CCDM was NOT hot-pressed, but physically laid upon the surface of the membrane so the only pressing they underwent was from the torqueing down of the cell hardware. This strategy ensured that the majority of the cathode electrocatalyst remained on the gas diffusion layer (GDL) after detachment from the membrane subjected to post-MEA testing.

MEA tests.—The MEAs with a size of 50 cm^2 were tested under H_2/O_2 following the suggested protocol issued by the Department of Energy (DOE):[17] H_2/O_2 with stoichiometries of 2.0 and 9.5, cell temperature of 80°C, 100% relative humidity, and a back pressure of 150 kPa_{abs}. The cell potential was swept at 50 $mV \cdot s^{-1}$ between 0.6 and 1.0 V (all potentials vs. reversible hydrogen electrode (RHE) unless otherwise stated) under O_2 in a triangular profile for up to 30,000 cycles. The MEAs were subjected to the cathode catalytic activity (H_2/O_2) performance tests after 200 (denoted as BOL (beginning of life)), 10,000 (denoted as MOL (middle of life)), and 30,000 (denoted as EOL (end of life)) voltage cycles. The data collection methods followed the guidelines set by the USCAR Fuel Cell Tech Team.[18]

Electrode preparation and XAS data collection.—Upon the completion of MEA testing, the cathode CCM with or without the membrane, the membrane alone, or the cathode CCDM were detached from the membrane and then mounted into a previously described spectro-electrochemical half-cell[19] for in situ XAS measurements. Multiple layers were necessary for the Co/Ni geometric loading to reach a ~0.05 edge height at the Co/Ni K edge. All data were collected in the fluorescence mode at the beamline X3B National Synchrotron Light Source (NSLS), and the beamline 8-ID at the NSLS-II, Brookhaven National Laboratory. The 0.1M $HClO_4$ electrolyte was constantly purged with either nitrogen or oxygen gases while being continuously pumped through the cell. The voltage cycling limits were 0.05 to 1.1 V vs. RHE. In situ XAS Data collection was conducted as a function of applied potentials during the anodic sweep to avoid the hysteresis effect;[20] At each potential the data was collected after the electrode surface reaching the steady state. To refresh the surfaces after each potential hold (i.e. clear off the catalytic surfaces of any accumulated oxygen species), the electrode was fully cycled after each potential hold until the voltammograms were stabilized.

XAS data analysis.—The data were processed and fitted using the IFEFFIT-based Athena[21] and Artemis[22] programs. Scans were calibrated, aligned and normalized with background removed using the IFEFFIT suite[23] (version 1.2.9, IFEFFIT Copyright 2005, Matthew Newville, University of Chicago, http://cars9.uchicago.edu/ifeffit/). The χ(R) were modeled using single scattering paths calculated by FEFF6.[24]

Results and Discussion

XAS characterizations on the single-sided CCM.—In order to unambiguously show that the XAS signals obtained even by the fluorescence mode is a bulk average of the signals from the electrode and the membrane, ex situ measurements were performed on the single-sided CCM MEAs at different cycling stage (0k – 30k voltage cycles between 0.6 – 1.0 V vs. RHE in PEMFCs). The single-sided CCM MEA subject to XAS measurements was formed by detaching the anode Pt/C electrode from the MEA, i.e. the membrane together with the cathode PtCo/C electrode. Afterwards, the membrane and cathode PtCo/C electrode were detached and subjected to XAS measurements separately. In addition, CoO and the fresh electrode composed of the same PtCo/C electrocatalyst used in the MEAs were measured as baseline materials for comparison.

Figure 1a presents the ex situ Co K-edge X-ray absorption near edge structure (XANES) spectra of the single-sided CCM MEAs at various cycling stages. The white line intensity of the XANES of the MEA increases with potential cycling (e.g. BOL < MOL < EOL), and that of the MEA at the EOL stage closely approaches that of the CoO. These data clearly show the increasing amount of Cobalt oxide (CoO_x)

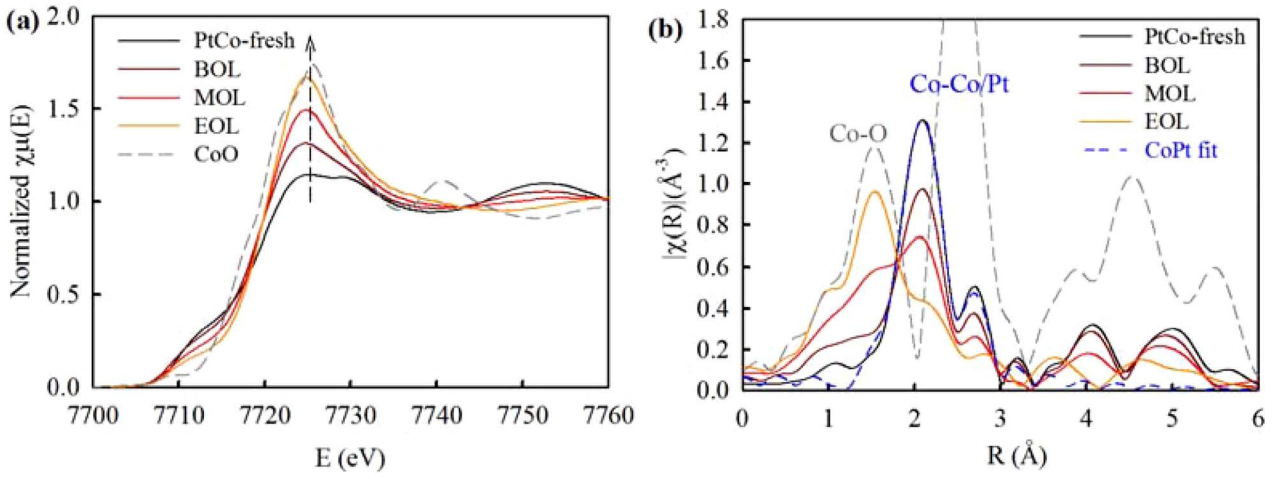

Figure 1. The Co K-edge XANES (a) and FT-EXAFS (b) spectra of the single-sided CCM MEAs collected at various cycling stages (BOL, MOL, and EOL) ex situ, together with the CoO standard and the fresh PtCo/C electrocalalyst used in the MEAs measured in an Ar-saturated 0.1 M $HClO_4$ electrolyte at 0.54 V in a spectro-electrochemical half-cell.

in the single-sided MEA with potential cycling. This trend is further supported by the Fourier transform of the extended X-ray absorption fine structure (FT-EXAFS) spectra (Figure 1b). The intensity of the FT-EXAFS peak around 1.5 Å (without phase correction) that arises from the Co-O scattering increases with potential cycling, which is accompanied by the decrease of the intensity of the FT-EXAFS peak around 2 Å. The fitting (blue dashed line) of the FT-EXAFS spectrum of the fresh PtCo/C electrode collected at 0.54 V in Ar-purged 0.1 M $HClO_4$ in a half-cell confirms that this peak is co-contributed by the Co-Co and Co-Pt scatterings as expected from the CoPt alloying phase. Therefore, the Co K-edge XANES, FT-EXAFS spectra, and a combination thereof verify that the relative content of the CoO_x increases with potential cycling; meanwhile the relative content of the CoPt alloying phase decreases. These trends indicate the gradual dealloying process of the PtCo/C electrocatalyst during long-term PEMFC operation, and the dealloyed Co presents in the form of oxide when exposed to air.

This gradual dealloying process of the PtCo/C electrocatalyst with the potential cycling in a PEMFC is also observed from the Pt perspective. The EXAFS fitting of the Pt L_3 edge spectra of the same single-sided MEA show that the number of the first shell Co neighbors decreases with potential cycling (Table I), which is manifested by the decreasing intensity of the Pt-Co scattering peak with potential cycling (Figure 2). At the EOL stage, the spectrum is dominated by the Pt-Pt scattering and the contribution from the Pt-Co scattering is minimal. This result is in line with the observation that the Co K-edge spectrum at the EOL stage is dominated by the signals of CoO_x, and a combination thereof suggests the nearly complete dealloying of the PtCo/C electrocatalyst at the EOL stage. Thus, the dealloying process with potential cycling is unambiguously confirmed from both Pt and Co perspectives. This phenomenon has been previously reported by Chen et al.[25] on the basis of microscopic characterizations on the PtCo/C electrocatalyst operated in MEAs, and even on Pt/C electrocatalysts without the second transition metal.[26] Large crystalline Pt and Co^{2+} species were found in the ionomer phase in both the membrane and the electrode, as a consequence of the PtCo/C dealloying followed by dissolution. Therefore, the XAS data collected on the single-sided MEA (Figures 1 and 2) at both Pt and Co edges are bulk averaged throughout the membrane, ionomer, and electrode. While the bulk average XAS data firmly verify the dealloying process, they

Table I. Summary of EXAFS results*.

scattering path	Cycling stage	bond length (Å)	coordination number	D-W factor ($Å^2$)
Pt-Pt	fresh	2.71(1)	6.3(9)	0.005(1)
	BOL	2.71(1)	5.2(7)	0.006(3)
	MOL	2.73(1)	7.0(6)	0.006(5)
	EOL	2.75(1)	8.3(7)	0.006(5)
Pt-Co	fresh	2.63(1)	2.0(7)	0.010(2)
	BOL	2.63(1)	2.2(5)	0.012(7)
	MOL	2.64(1)	1.5(4)	0.012(6)
	EOL	2.66(1)	0.6(3)	0.012(6)

*The data of the PtCo-fresh were collected at 0.54 V vs RHE in an O_2-saturated 0.1 M $HClO_4$ electrolyte. $S_0{}^2$ fixed at 0.766 for Pt as obtained by fitting the reference foil. Fits were done in *R*-space, $k^{1,2,3}$ weighting at the Pt L_3-edge with the windows of $1.1 < R < 3.4$ Å and $\Delta k = 2.95 - 12.14$ $Å^{-1}$ The ΔE values is 7.3 ± 1.0 eV. Values given in parentheses represent statistical errors of the least-squares fits determined by ARTEMIS.

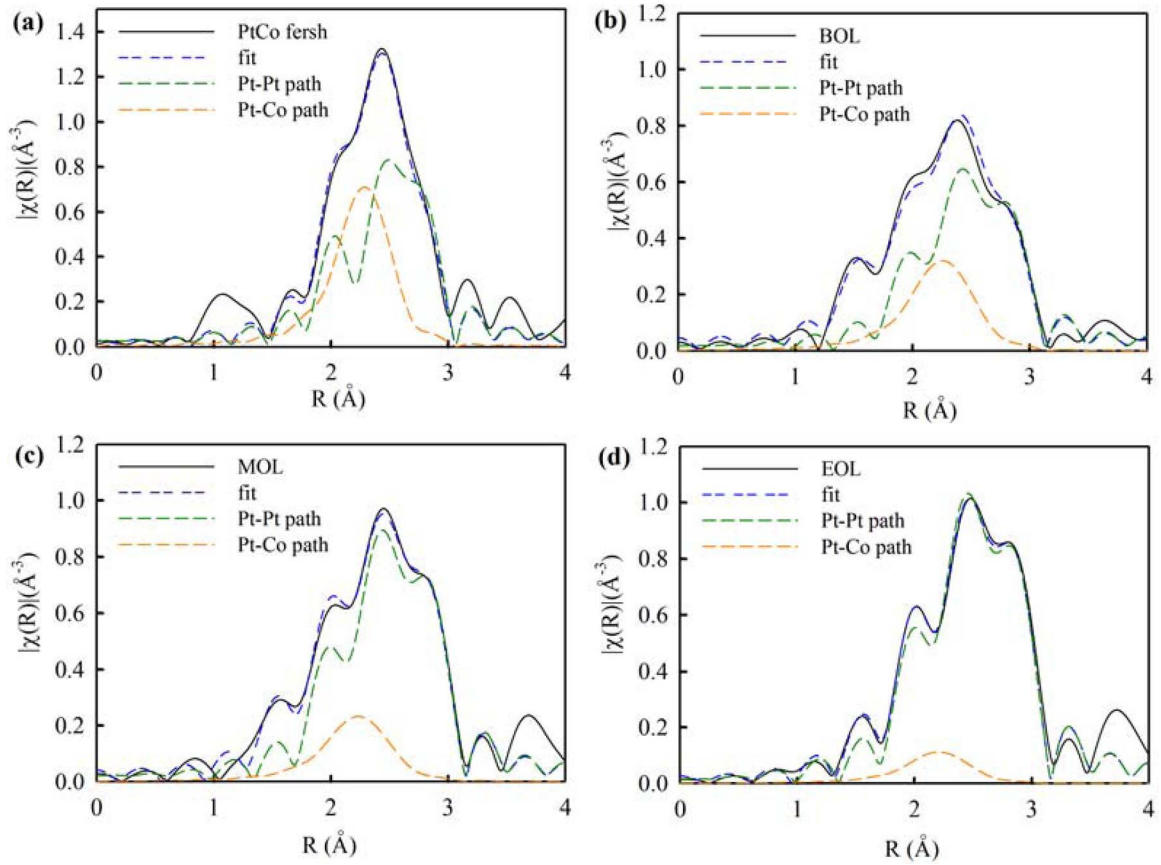

Figure 2. The Pt L_3-edge FT-EXAFS spectra and the corresponding fitting of the single-sided CCM MEAs at (b) BOL, (c) MOL (b), (d) EOL, and (a) the PtCo/C fresh electrode measured in an Ar-saturated 0.1 M $HClO_4$ electrolyte at 0.54 V in a spectro-electrochemical half-cell for comparison.

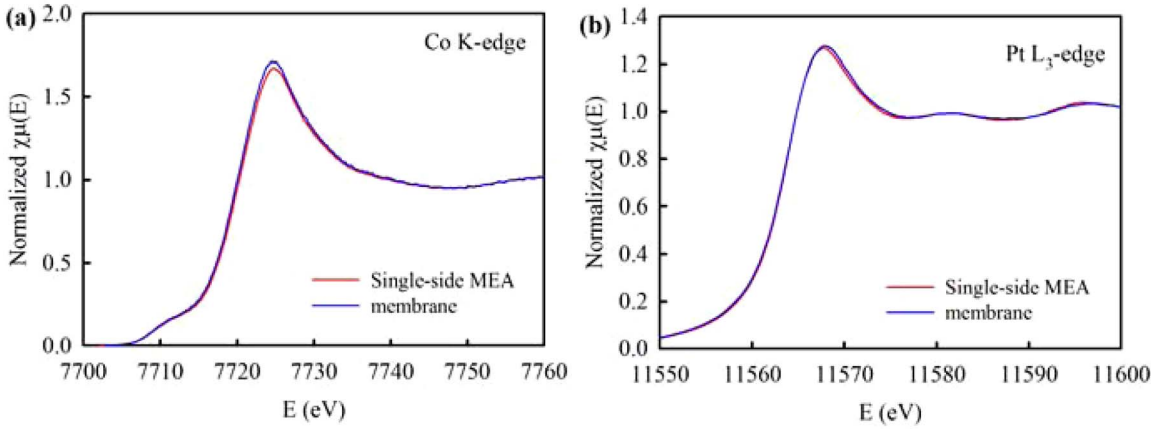

Figure 3. The XANES of the Co K-edge (a) and Pt L_3-edge (b) spectra of the single-sided CCM MEAs and the membrane detached from the MEA at the EOL stage.

cannot be directly related to the morphology of the electrocatalyst in the electrode. It is noted that the CoO_x is observed even at the BOL stage (200 cycles) (Figure 1), which indicates that the dissolution of Co occurs at the very early stage of potential cycling. The lack of the long range order of the CoO_x, which is evidenced by the absence of the Co-Co scattering around 2.5 Å and any peaks further featured by CoO, indicates that the CoOx in the membrane and/or ionomer is highly amorphous. In addition to Co, significant amount of Pt is also dissolved upon long-term PEMFC operation and migrates into the membrane forming large single crystalline Pt,[25,26] and its XAS signal cannot be separated from the XAS signals from the cathode electrode. The dissolved species in the membrane and the ionomer are electrically disconnected and thus electrochemically inactive.[25] Therefore, operando XAS characterization on MEAs is seriously limited by this issue throughout the whole potential cycling stage with the aim of providing the structural and electronic properties of the electrocatalyst under working conditions.

In order to exclusively probe the structure of the PtCo/C electrocatalyst in the electrode, the electrode was detached from the membrane and then transferred into the half-cell for in situ XAS measurements. The major advantage of this strategy is that the electrode was cycled in a practical PEMFC rather than in a half-cell, and thus provides more relevant spectroscopic data to the degradation in PEMFCs.[9] However, no XAS signals were detected at both the Pt and Co edges. On the other hand, the XAS spectra of the membrane are close to those of the single-sided MEA (Figure 3). These results show that the vast majority of the PtCo/C powders were remained on the membrane rather than on the electrode upon the detachment. This can be related to the CCM fabrication method wherein the electrocatalyst was coated on the surface of the membrane, and eventually became a physically intimate part of the membrane upon the subsequent hot press. Therefore, the dissolved species in the membrane and the electrocatalyst in the electrode cannot be separated for the MEA fabricated via the CCM method.

XAS characterizations on the CCDM cathode electrocatalyst.— The aforementioned difficulty was overcome by the collaborating efforts between us and General Motors by adopting the CCDM method for MEA fabrication (detailed information provided in the Experimental Section). In brief, the electrocatalyst was coated on the microporous layer rather than the membrane, and then the cathode was physically laid on the surface of the membrane without hot-pressing. As a consequence, the majority of the electrocatalyst powders were remained on the GDL upon the detachment from the membrane, and multiple layers of GDL were transferred to the half-cell for in situ XAS measurements. As shown below, the feasibility of this strategy is demonstrated by measuring the dealloyed PtNi/C electrocalysts that exhibited the record ORR activity and durability in PEMFCs.[15]

The XAS spectra were acquired at both the Ni K-edge and Pt L_3-edge for the dealloyed PtNi/C electrodes detached from the CCDM-fabricated MEAs subjected to BOL, MOL, and EOL cycling stages (Figure 4). The decent quality of the data is manifested by the signals in the energy space (Figures 4a and 4c) and K space (Figures 4b and 4d). These data confirm that sufficient powders were retained on the GDL rather than on the membrane upon detachment from the MEA, opposite to the case of the CCM-fabricated MEAs. This constitutes a prerequisite for in situ XAS characterizations on *PEMFC-cycled* electrolcatalysts.

The major merit of this method lies in the separation of the electrocatalyst retained on the electrode from the dissolved species in the membrane during long-term PEMFC operation. The drastic increase of the Pt/Ni atomic ratio from 2.2 at the BOL stage to 7.6 at the EOL stage (determined by the electron probe microanalysis (EPMA)) indicates that significant amount of Ni was dissolved during long-term PEMFC operation. Despite so, the white line intensity of the Ni XANES does not increase with potential cycling (Figure 4a). This suggests that no Ni oxides are remained in the detached GDL and the ionomer throughout the whole potential cycling stage; otherwise the white line intensity would increase with cycling as observed on the single-sided MEA (Figure 1a). The absence of Ni oxides is not surprising since the majority of the Ni oxides were located in the membrane; Ni oxides retained on the GDL and the ionomer, if there is any, will quickly dissolve in the acidic electrolyte of 0.1 M $HClO_4$. The absence of Ni oxides in the electrode is further confirmed by performing the EXAFS fitting of the spectra of the PtNi/C at the Ni and Pt edges simultaneously. Fitting results are listed in Table II. As shown in Figure 5, no FT-peaks arisen from the Ni-O scattering around 1.5 Å were presented in the FT-EXAFS spectra at all three cycling stages, and the spectra can be well fitted with two Ni-Ni and Ni-Pt scattering vectors (the right side of Figure 5 and Table II). In addition, the absence of the Pt-O scattering at 0.54 V revealed by the fitting indicates that the amount of the Pt trapped in the ionomer, which is in the form of oxides,[25] is insignificant compared to the Pt in the GDL.

In addition to verifying the absence of the Ni oxides in the electrode, the EXAFS fitting confirms that the XAS signals arise exclusively from the PtNi/C electrocatalyst cycled in a PEMFC. Direct evidence for that is the linear correlation between the bulk average first shell Pt-Pt bond length (R_{PtPt}) determined by the EXAFS fittings and the Ni content given by EPMA, as per Vegard's law (Figure 6). Meanwhile, the R_{NiNi} of the PtNi/C electrocatalyst throughout the whole potential cycles remains nearly unchanged, and perfectly matches the R_{NiNi} (2.572 Å) derived from Vegard's law based on the Ni relative content in the $PtNi_3$ precursor (75%) (Figure 6). The combination of the trends of R_{PtPt} and R_{NiNi} with potential cycling depicts that the core of the PtNi/C carries the $PtNi_3$ phase from the $PtNi_3$ precursor and remains intact during long-term PEMFC operation, whereas the

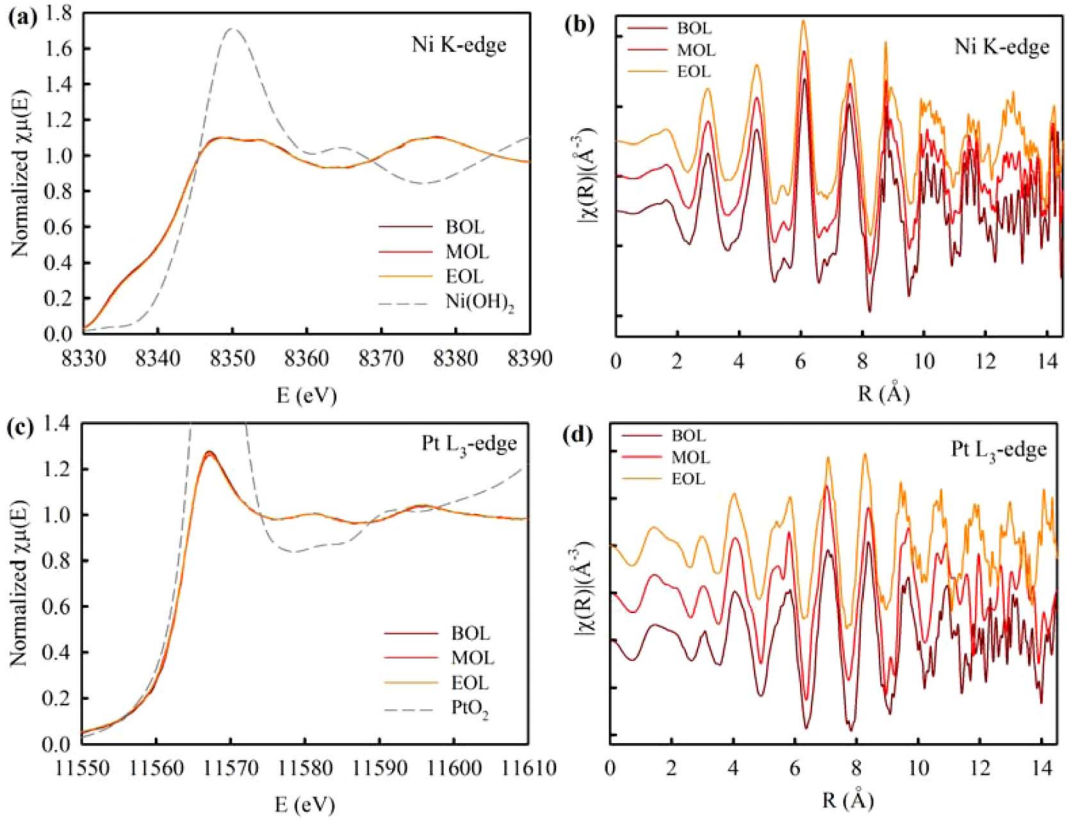

Figure 4. The Ni K-edge (top) and Pt L_3-edge (bottom) spectra of the dealloyed PtNi/C electrocatalyst CCDM electrode detached from the MEA subjected to various extent of potential cycling (BOL, MOL, and EOL) in energy space (left) and K space (right). The spectra were collected in an O_2-saturated 0.1 M $HClO_4$ electrolyte at 0.54 V in a spectro-electrochemical half-cell. The spectra of $Ni(OH)_2$ and PtO_2 were also presented for comparison.

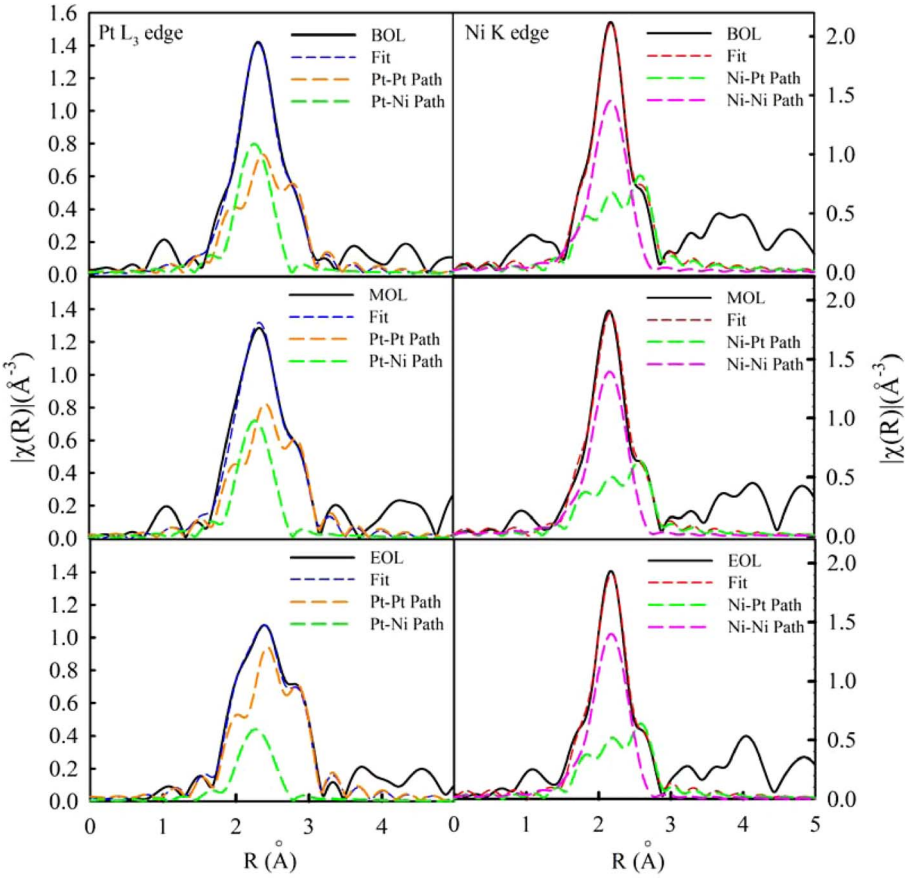

Figure 5. The Pt L_3 edge (left) and Ni K edge (right) EXAFS spectra of the dealloyed PtNi/C electrode at various potential cycling stages of BOL (top), MOL (middle), and EOL (bottom) collected at an 0.54 V in O_2-saturated 0.1 M $HClO_4$ electrolyte, and the corresponding least-squares fits.

Table II. Summary of EXAFS results*.

scattering path	Cycling stage	bond length (Å)	coordination number	D-W factor (Å^2)
Pt-Pt	BOL	2.696(6)	7.3(7)	0.007(4)
	MOL	2.716(6)	8.2(6)	
	EOL	2.740(5)	9.7(7)	
Pt-Ni	BOL	2.602(6)	2.5(5)	0.005(4)
	MOL	2.607(8)	2.2(6)	
	EOL	2.607(4)	1.3(7)	
Ni-Pt	BOL	2.602(6)	4.8(6)	0.005(4)
	MOL	2.607(8)	3.8(6)	
	EOL	2.607(4)	3.7(7)	
Ni-Ni	BOL	2.574(5)	7.7(5)	0.011(6)
	MOL	2.575(6)	7.4(5)	
	EOL	2.574(4)	7.4(3)	

*All the data were collected at 0.54 V (double layer region) in an O_2-saturated 0.1 M $HClO_4$ electrolyte. S_0^2 fixed at 0.766 and 0.682 for Pt and Ni, respectively as obtained by fitting the reference foils. Fits were done in *R*-space, $k^{1,2,3}$ weighting at Pt L_3 and Ni k edges simultaneously. For Pt, $1.1 < R < 3.4$ Å and $\Delta k = 2.95 - 12.14$ Å^{-1} were used; for Ni, $1.2 < R < 3.0$ Å and $\Delta k = 1.87 - 11.93$ Å^{-1} were used. The ΔE values of the Ni K and Pt L_3 edges are -4.3 ± 0.5 and 6.1 ± 0.6 eV, respectively. Values given in parentheses represent statistical errors of the least-squares fits determined by ARTEMIS. The Pt-Ni and Ni-Pt bond distances were set to be identical during the fitting.

outer shells relax as a result of the Ni dissolution from the outer shell (Figure 6). The selective dealloying and dissolution of the Ni from outer shells is also reflected by the combined results that the coordination numbers of the Pt-Ni and Ni-Pt reduce with potential cycling whereas that of Ni-Ni remains largely constant (Table II). The increase of the R_{PtPt} caused by the dissolution of Ni during long-term PEMFC operation directly verifies the gradual attenuation of the compressive-strain, which has been widely acknowledged as the main factor of the performance degradation of the PtM/C electrocatalyst during long-term PEMFC operation.[25,27,28] These experimental data therefore justify the feasibility of our method of the in situ XAS characterization on the PEMFC-cycled Pt-electrodes.

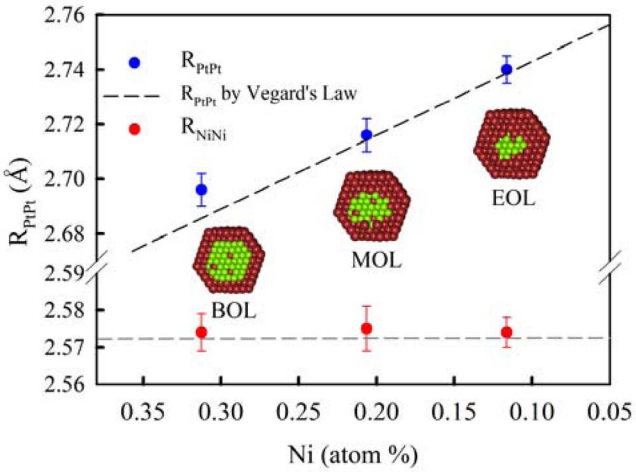

Figure 6. The experimental R_{PtPt}(s) (blue dots) of the PtNi/C at BOL, MOL, and EOL stages in comparison to those calculated using the Ni atomic content obtained by EPMA as per Vegard's Law (black dashed line); The experimental R_{NiNi}(s) (red dots) in comparison with the R_{NiNi} (gray dashed line) calculated using the Ni relative content in the precursor (0.75) as per Vegard's law.

Conclusions

In this work, we demonstrated that operando *XAS* characterizations on the PEMFC-cycled PtM/C electrocatalysts is technically challenging due mainly to the convolution of the XAS signals from the PtM/C retained in the electrode and the dissolved Pt and M species in the membrane upon long-term PEMFC operation. We overcome this difficulty by developing the CCDM method for the MEA fabrication. This method enables a clean separation of the PtNi/C electrocatalyst retained in the electrode from the dissolved species in the membrane, and thus allows for in situ XAS characterization on the electrode cycled in PEMFCs. The difficulty revealed here is not captive to XAS, but rather a common issue for spectroscopic techniques with bulk-average nature. The method developed here can be readily extended to these techniques to characterize materials tested in fuel cells and batteries under working conditions. While this method is a step forward in terms of in situ XAS characterizations, operando XAS characterizations of the electrode in practical devices is still the ultimate goal. This may be feasible in the future if the dissolved species can be removed from the membrane in a fuel cell without disassembling the MEA and XAS spectra can be collected by quick-XAS before the membrane being contaminated by the dissolved species upon reoperation of a fuel cell.

Acknowledgment

This research was supported by the Fuel Cell Technology Program of the Office of Energy Efficiency and Renewable Energy of the U.S. Department of Energy under contract DE-EE0000458. The catalyst precursors were provided by R.O'Malley and A. Martinez (Johnson Matthey). Joseph M. Ziegelbauer, Ratandeep S. Kukreja, Anusorn Kongkanand performed the MEA fabrication and MEA tests. Use of the beamline X3B of the National Synchrotron Light Source (NSLS-I), and ISS 8-ID of the NSLS II was supported by the National Synchrotron Light Source (NSLS) II, Brookhaven National Laboratory, under U.S. DOE Contract No. DE-SC0012704. Brookhaven National Laboratory was supported by the U.S. Department of Energy, Office of Science, Office of Basic Energy Sciences, under Contract No. DE-AC02-98CH10886. This publication was made possible by the Center for Synchrotron Biosciences grant, P30-EB-009998, from the National Institute of Biomedical Imaging and Bioengineering (NBIB).

ORCID

Todd E. Miller https://orcid.org/0000-0001-8592-8008
Qingying Jia https://orcid.org/0000-0002-4005-8894

References

1. P. Strasser, S. Koh, T. Anniyev, J. Greeley, K. More, C. Yu, Z. Liu, S. Kaya, D. Nordlund, and H. Ogasawara, *Nat. Chem.*, **2**, 454 (2010).
2. V. R. Stamenkovic, B. Fowler, B. S. Mun, G. Wang, P. N. Ross, C. A. Lucas, and N. M. Marković, *Science*, **315**, 493 (2007).
3. F. Calle-Vallejo, M. D. Pohl, D. Reinisch, D. Loffreda, P. Sautet, and A. S. Bandarenka, *Chem. Sci.*, **8**, 2283 (2017).
4. M. Li, Z. Zhao, T. Cheng, A. Fortunelli, C.-Y. Chen, R. Yu, Q. Zhang, L. Gu, B. V. Merinov, Z. Lin, E. Zhu, T. Yu, Q. Jia, J. Guo, L. Zhang, W. A. Goddard, Y. Huang, and X. Duan, *Science*, **354**, 1414 (2016).
5. Q. Jia, K. Caldwell, K. Strickland, J. M. Ziegelbauer, Z. Liu, Z. Yu, D. E. Ramaker, and S. Mukerjee, *ACS Catal.*, **5**, 176 (2015).
6. Q. Jia, J. Li, K. Caldwell, D. E. Ramaker, J. M. Ziegelbauer, R. S. Kukreja, A. Kongkanand, and S. Mukerjee, *ACS Catal.*, **6**, 928 (2016).
7. X. Huang, Z. Zhao, L. Cao, Y. Chen, E. Zhu, Z. Lin, M. Li, A. Yan, A. Zettl, Y. M. Wang, X. Duan, T. Mueller, and Y. Huang, *Science*, **348**, 1230 (2015).
8. J. C. Meier, I. Katsounaros, C. Galeano, H. J. Bongard, A. A. Topalov, A. Kostka, A. Karschin, F. Schuth, and K. J. J. Mayrhofer, *Energy Environ. Sci.*, **5**, 9319 (2012).
9. Q. Jia, W. Liang, M. K. Bates, P. Mani, W. Lee, and S. Mukerjee, *ACS Nano*, **9**, 387 (2015).
10. Q. Jia, K. Caldwell, D. E. Ramaker, J. M. Ziegelbauer, Z. Liu, Z. Yu, M. Trahan, and S. Mukerjee, *J. Phys. Chem. C*, **118**, 20496 (2014).
11. J. Li, A. Alsudairi, Z.-F. Ma, S. Mukerjee, and Q. Jia, *J. Am. Chem. Soc.*, **139**, 1384 (2017).

12. Q. Jia, E. Lewis, C. Grice, E. Smotkin, and C. Segre, *J. Phys. Conf. Ser.*, **190**, 012157 (2009).
13. E. A. Lewis, I. Kendrick, Q. Jia, C. Grice, C. U. Segre, and E. S. Smotkin, *Electrochim. Acta*, **56**, 8827 (2011).
14. S. Mingfeng, Z. Tiantian, B. Hongliang, D. Peiquan, L. Rui, H. Yuying, and W. Jianqiang, *Nuclear Techniques*, **39**, 60101 (2016).
15. B. Han, C. E. Carlton, A. Kongkanand, R. S. Kukreja, B. R. Theobald, L. Gan, R. O'Malley, P. Strasser, F. T. Wagner, and Y. Shao-Horn, *Energy Environ. Sci.*, **8**, 258 (2015).
16. J. C. Doyle, B. Sompalli, and S. G. Yan, Durable membrane electrode assembly catalyst coated diffusion media with no lamination to membrane, in, Google Patents (2005).
17. *DOE, Hydrogen and Fuel Cell Activities, Progress, and Plans*, in *Report to Congress*, U. S. D. O. Energy Editor, p. 43, United States Department of Energy, Washington D.C. (2009).
18. A. Kongkanand and F. Wagner, *Annual Merit Review, US Department of Energy Hydrogen and Fuel Cells Program*, in (2014).
19. T. M. Arruda, B. Shyam, J. S. Lawton, N. Ramaswamy, D. E. Budil, D. E. Ramaker, and S. Mukerjee, *J. Phys. Chem. C*, **114**, 1028 (2009).
20. K. Sasaki, N. Marinkovic, H. S. Isaacs, and R. R. Adzic, *ACS Catal.*, **6**, 69 (2016).
21. M. Newville, *J Synchrotron Radiat.*, **8**, 322 (2001).
22. B. Ravel and K. Gallagher, *Phys. Scr.*, **2005**, 606 (2005).
23. M. Newville, P. Limacrvincedilscaron, Y. Yacoby, J. J. Rehr, and E. A. Stern, *Phys. Rev. B*, **47**, 14126 (1993).
24. A. L. Ankudinov, B. Ravel, J. J. Rehr, and S. D. Conradson, *Phys. Rev. B*, **58**, 7565 (1998).
25. S. Chen, H. A. Gasteiger, K. Hayakawa, T. Tada, and Y. Shao-Horn, *J. Electrochem. Soc.*, **157**, A82 (2010).
26. H. Schulenburg, B. Schwanitz, J. Krbanjevic, N. Linse, G. G. Scherer, and A. Wokaun, *Electrochem. Commun.*, **13**, 921 (2011).
27. Q. Jia, K. Caldwell, J. M. Ziegelbauer, A. Kongkanand, F. T. Wagner, S. Mukerjee, and D. E. Ramaker, *J. Electrochem. Soc.*, **161**, F1323 (2014).
28. H. A. Gasteiger, S. S. Kocha, B. Sompalli, and F. T. Wagner, *Appl. Catal. B-Environ.*, **56**, 9 (2005).